Secondary ion mass spectrometry quantification of boron distribution in an array of silicon nanowires

Pawel Piotr Michalowski, Jonas Müller, Chiara Rossi, Alexander Burenkov, Eberhard Bär, Guilhem Larrieu, Peter Pichler

▶ **To cite this version:**

Pawel Piotr Michalowski, Jonas Müller, Chiara Rossi, Alexander Burenkov, Eberhard Bär, et al.. Secondary ion mass spectrometry quantification of boron distribution in an array of silicon nanowires. Measurement - Journal of the International Measurement Confederation (IMEKO), 2023, 211, pp.112630. 10.1016/j.measurement.2023.112630 . hal-04234520

HAL Id: hal-04234520
https://laas.hal.science/hal-04234520v1

Submitted on 10 Oct 2023

HAL is a multi-disciplinary open access archive for the deposit and dissemination of scientific research documents, whether they are published or not. The documents may come from teaching and research institutions in France or abroad, or from public or private research centers.

L'archive ouverte pluridisciplinaire **HAL**, est destinée au dépôt et à la diffusion de documents scientifiques de niveau recherche, publiés ou non, émanant des établissements d'enseignement et de recherche français ou étrangers, des laboratoires publics ou privés.

Measurement 211 (2023) 112630

Contents lists available at ScienceDirect

Measurement

journal homepage: www.elsevier.com/locate/measurement

Secondary ion mass spectrometry quantification of boron distribution in an array of silicon nanowires

Paweł Piotr Michałowski [a,*], Jonas Müller [b], Chiara Rossi [c], Alexander Burenkov [c], Eberhard Bär [c], Guilhem Larrieu [b], Peter Pichler [c]

[a] Łukasiewicz Research Network - Institute of Microelectronics and Photonics, Aleja Lotników 32/46, 02-668 Warsaw, Poland
[b] LAAS-CNRS, Université de Toulouse, Toulouse, 31031, France
[c] Fraunhofer Institute for Integrated Systems and Device Technology IISB, 91058 Erlangen, Germany

ARTICLE INFO

Keywords:
Secondary ion mass spectrometry
SIMS
Nanowires
Gate-all-around
Boron
Segregation

ABSTRACT

The development of non-planar structures such as arrays of nanowires (NWs), poses a significant challenge for dopant concentration determination. Techniques that can be readily used for 3D structures usually lack the desired sensitivity whereas secondary ion mass spectrometry (SIMS), known for its excellent detection limits, is designed to analyze flat samples. In this work, we overcome the limitation of standard SIMS approaches. NWs are covered with photoresist forming a flat surface. For high incident angle bombardment, the sputtering process becomes self-flattening, i.e. the ions collide with the sidewalls of the exposed tips of NWs at much lower angles and sputter them significantly faster. Thus, reliable information about the dopant distribution along the height of NWs can be obtained. The SIMS analysis can be performed on an array of 1000 x 1000 nanowires with a detection limit of about 5 x 10^{16} atoms/cm^3 and a reasonable signal-to-noise ratio of about 10 dB.

1. Introduction

Nanowires (NWs) are receiving global recognition due to their quasi-one dimensional geometry and resulting unique properties, such as high area-to-volume ratio, high optical output, low defect density, and waveguiding properties [1–3]. Their potential applications are ranging from photonics [4], electronics [5], optoelectronics [6], sensing [7], photovoltaics [8], and energy storage [9], to name just a few.

To further develop NWs based devices it is essential to assess their chemical composition, particularly dopant distribution. For uniformly doped NWs charge concentration can be determined using Kelvin probe force microscopy [10], photoluminescence [10], Raman spectroscopy [11] or off-axis electron holography [12]. However, most of these techniques have poor detection limits.

Additional complications arise when the dopant distribution in not uniform. One such example is an array of boron-doped silicon NWs which are fabricated in a top-down manner by patterning and anisotropic etching of a doped silicon substrate [13–15]. To fabricate the gate-all-around nanowire field-effect transistors (GAA-NW-FETs) several oxidation processes are usually performed [16,17]. Wet-thermal oxidation, or a prolonged dry-thermal oxidation, and subsequent oxide removal are used to obtain the desired NW diameter also creating a new defect-free interface [18]. Finally, a short dry oxidation creates a thin gate oxide. It is well known that during these oxidation processes boron atoms preferentially segregate into the growing oxide and, thus, the concentration in the remaining silicon core may significantly decrease [19–21].

Atom probe tomography (APT) may be considered a perfect candidate to analyze dopant distributions in a nanowire, particularly because the shape of a sample is already similar to the tip-shaped specimen used in the APT analysis. It should be, however, noted that most APT analyses of p-type silicon have been performed on samples with boron concentrations exceeding 10^{20} atoms/cm^3 and the background/noise level is usually in the order of 1–2 x 10^{19} atoms/cm^3 [22–24]. For the GAA-NW-FET device much lower concentrations are required and, thus, APT analysis becomes not feasible. Furthermore, the sample preparation and analysis are both time-consuming and performed on a single NW, not a full array.

On the other hand, secondary ion mass spectrometry (SIMS) provides a much bigger analysis area and is well-known for its excellent detection limits of trace elements [25–30], even in the 10^{12} atoms/cm^3 range [30]. Particularly, SIMS profiling of boron dopants is widely discussed in metrology-related journals and proceedings of SIMS conferences for more than forty years [31–38]. However, standard SIMS analysis is performed on a flat sample and cannot be directly used

* Corresponding author.
E-mail address: pawel.michalowski@imif.lukasiewicz.gov.pl (P.P. Michałowski).

https://doi.org/10.1016/j.measurement.2023.112630
Received 20 December 2022; Received in revised form 4 February 2023; Accepted 17 February 2023
Available online 23 February 2023
0263-2241/© 2023 The Author(s). Published by Elsevier Ltd. This is an open access article under the CC BY license (http://creativecommons.org/licenses/by/4.0/).

to characterize 3D nanostructures (cf. Figure S1 in Supplementary Materials).

In this work, we present a procedure to overcome this limitation. Prior to the measurement silicon NWs are embedded in organic material. In standard SIMS, the difference in the etching rate of these materials would result in a non-uniform sputtering process. However, high incident angle bombardment ensures that the sputtering process is self-flattening, i.e. when the tips of NWs are exposed, the incoming primary ions collide with the sidewalls of the NWs directly and thus these tips are sputtered much faster than the organic material. The result of a measurement recreates the distribution of boron along the height of NWs.

2. Experimental setup

2.1. Sample preparation

Large Arrays of vertical nanowires (100 × 100) were fabricated by a top down approach on highly doped p-type silicon (boron-doped at 3.88×10^{19} cm^3) [39–41]. An initial mask of a negative-tone resist (hydrogen sylesquioxane) was patterned on the substrate through low voltage (30 kV) electron beam lithography using a Raith-150 system. The highly vertical nanopattern was successively transferred into the substrate by fluorine-based anisotropic reactive ion etching in an Alcatel AMS4200 system, creating perfectly vertical nanostructures of 270 nm height. The remaining resist was removed in diluted hydrofluoric acid, followed by a low-power oxygen plasma cleaning step. The as-fabricated NWs were then oxidized by either wet- or dry-thermal oxidation in a Centronic E1550HT tube furnace. Wet-thermal oxidation was carried out at 850 °C for 5 min to create 20.6 nm of oxide while an equally thick oxide layer of 19.2 nm could be achieved through dry oxidation at 860 °C for 66 min. This sacrificial oxide layer was removed by wet chemical etching in a buffered oxide etchant, reducing the size of the NWs. Finally, a thin dry-oxide layer of few nm was created by dry-thermal oxidation at 725 °C for 20 min and removed in buffered oxide etchant. All samples, having undergone the exactly same structuring process (lithography & etching) but different oxidation procedures, were embedded in an organic photoresist Microposit S1805. A thick layer of several hundred nm was spin-coated on the samples and etched down in an oxygen plasma until the surface was approximately 20 nm above the NWs' heads.

2.2. Secondary ion mass spectrometry

A CAMECA IMS SC Ultra instrument was used in all experiments. The incident angle of the cesium primary beam was varied between 20 and 75°. The instrument did not allow direct control over the incident angle but different values could be achieved by changing voltages applied to the accelerator, sample holder, and the floating voltage applied to the primary column. The impact energy was 500 eV while the primary current was 10 nA, and the beam was rastered over 150 × 150 μm^2 whereas the analysis area was limited to 70 × 70 μm^2. Positive detector polarity was used and thus all signals were registered as CsX^+ cluster ions. Quantification was based on ion-implanted reference samples.

2.3. Complementary characterization techniques

Scanning electron microscopy (SEM) micrographs were obtained with a FEI Helios 600i double beam system to inspect samples before and after the photoresist deposition to determine the size of the NWs.

Atomic force microscopy (AFM) measurements were performed by a Bruker Dimension FastScan with ScanAsyst using silicon probes (Bruker OTESPA-R3 model) with a typical nominal tip radius of 7 nm. The depth of SIMS craters was determined and the root-mean-square (RMS) roughness of the samples was measured over a scan area of 30 × 30 μm^2.

Table 1
A summary of samples used in the experiment.

Name	Oxidation	Temperature (°C)	Time (min)	NW diameter (nm)	NW height (nm)
After etching	–	–	–	70	270
Dry	Dry	860	66	60	240
Wet	Wet	850	5	58	247
Gate	Wet	850	5		
	+ dry	725	20	53	241

3. Results and discussion

Fig. 1 presents a scanning electron microscopy (SEM) overview of the array of as-fabricated NWs confirming their high quality and uniformity. As mentioned, arrays of NWs usually undergo several oxidation processes and, thus, a series of samples is needed to evaluate boron segregation during each step. Four different arrays of NWs will be considered, as presented in Table 1.

It is important to emphasize that the lateral resolution of the SIMS technique is not enough to distinguish the oxidized and not oxidized parts of the NWs and, thus, the oxide has always been removed before the analysis (even the gate oxide). In this way, it is possible to assess the distribution of boron that remains in the silicon core of a nanowire.

Even though many SIMS instruments are equipped with position-sensitive detectors, it is impossible to perform a direct measurement on NWs. The ion bombardment of the three-dimensional structures leads to a non-uniform and impossible to predict sputtering process and thus the secondary ions would be emitted simultaneously from the substrate and the NWs (along their full height). A hypothetical solution would be to fill the space between the nanowires of NWs with undoped silicon forming a flat sample - a depth profile would reflect the distribution of dopant along the height of NWs. However, it is not feasible to uniformly deposit silicon, avoiding forming voids and rough surfaces. It is, however, possible for organic materials such as photoresists, as shown as set-in in Fig. 1. Unfortunately, a significantly different etching rate of these materials would once again result in a non-uniform sputtering process.

It should be, however, noted that the etching rate depends not only on the material but also on the incident angle of the primary ions, and, thus, additional experiments have been devised — for each incident angle silicon and S1805 photoresist material has been sputtered for 20 min and the depth of the crater has been measured with AFM, hence the sputtering rate has been calculated, as presented in Fig. 2A. It can be immediately noted that:

- For all incident angles the etching rate of the photoresist is almost an order of magnitude higher than for silicon;
- The etching rate does not change significantly in the range of 20–55° for both materials and starts to decrease for higher angles;
- For the 75° incident angle the etching rate of both materials decreased more than two orders of magnitude.

It can be therefore concluded that for the 75° incident angle the etching rate of the photoresist is more than an order of magnitude lower than for silicon in standard incident angles (20–55°). Thus, the sputtering process for 75° incident angle may be considered self-flattening, as schematically shown in Fig. 2B. Due to a much higher etching rate of the photoresist, at some point, the tips of the NWs will be exposed. However, the primary ions will collide with the sidewalls of the exposed NWs at much smaller angles and thus they will be etched much faster than the remaining photoresist and the sample will become flat again. A depth profile obtained in such non-trivial conditions will reflect the boron distribution along the height of the NWs.

To verify the self-flattening property of the measurement procedure AFM topography scans have been performed at the surface of a sample, and after sputtering of 10, 175, and 350 nm, i.e. still in the photoresist,

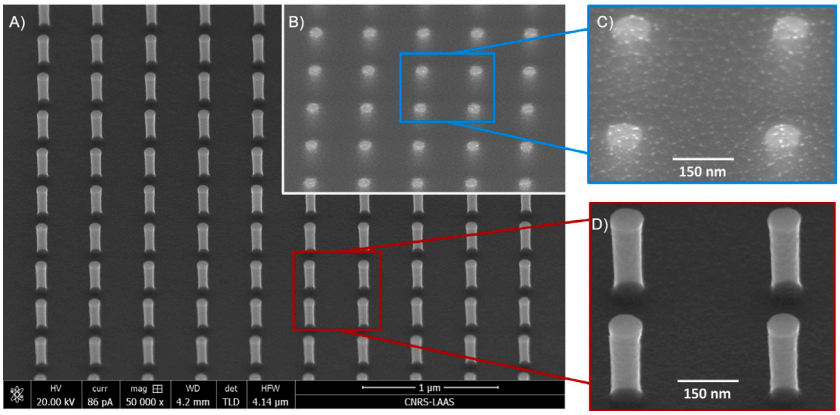

Fig. 1. SEM micrographs of large Si-nanowire arrays (100 × 100) after their top-down fabrication, using electron beam lithography and highly anisotropic reactive ion etching (Part A and D) and after embedding in an organic resist matrix (Part B and C).

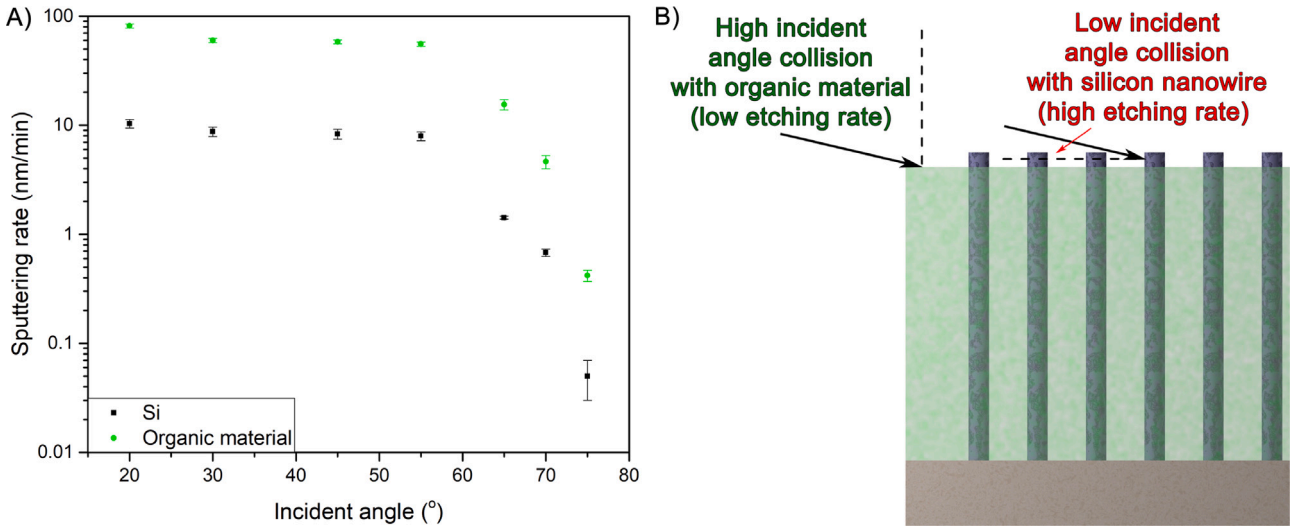

Fig. 2. Part A: the sputtering rate of silicon and organic material determined for different primary ions incident angles. Each data point is based on six separate measurements. Part B: the schematic concept of the self-flattening analysis. If the tips of NWs are exposed, the primary ions will collide with them at a much lower angle and sputter them at a much faster rate than the rest of the sample.

in the middle of NWs, and in the substrate, respectively. The resulting RMS roughness is 1.20, 0.92, 1.11, and 0.82 nm, respectively. It can be noted that the roughness decreases after the sputtering of 10 nm of photoresist and increases after reaching the NWs but it is still lower than at the surface of the sample. The lowest value has been obtained for the silicon substrate. AFM topography images are presented in Figures S2–5 in the Supplementary Materials.

As shown in Fig. 3A, a matrix effect and/or agglomeration of cesium at the interface between the organic material and the silicon results in artificial enhancements of the $CsSi^+$ and CsB^+ signals. To obtain the realistic distributions it is essential to perform point-to-point normalizations to the Cs^+ signal, as shown in Fig. 3B.

The analysis of the point-to-point normalized silicon signals yields important information about the validity of the method. As it is shown in Fig. 4A, the intensity of the silicon and boron signals coming from the substrate are the same for all samples but differ for the NWs region. The intensities of signals coming from the substrate correspond to the total field of view which has been set to $70\times70\ \mu m^2$. The intensity of the silicon signal coming from the NWs scales linearly with the total area of the NWs in the array and, thus, it is possible to determine the diameter of the NWs directly from the SIMS measurements. It equals 70.1 ± 0.6, 59.9 ± 0.7, 57.8 ± 0.7, and 52.9 ± 0.8 nm for samples after etching, as well as after dry, wet, and gate oxidations, respectively. These values are in perfect agreement with the actual size of the NWs, as presented in Table 1.

The change of the boron concentration from the tips of the NWs towards and into the substrate is presented in Fig. 4B. As expected, for the sample after etching there is no difference between NWs and the substrate regions but a clear depletion is observed for other samples, reaching up to about 200 nm into the substrate for the dry oxidized sample. Not surprisingly, the effect is significantly more pronounced for NWs as boron atoms can segregate into the growing oxide from all directions whereas the resupply of dopant from the bulk is less effective. Table 2 summarizes how much lower the boron concentration is on average and at the tip, middle (approximately 120 nm of height), and foot of the NWs when compared to the as fabricated NWs. The average ratio is ranging from 4.6 to 21.0 and the effect is significantly more pronounced at the tip of the NWs (ranging from factor 6.6 to 56.7).

It can be noted that the boron concentration is constant at the depths of 150–250 nm (NWs region) and 550–650 nm (substrate region) for all samples. Thus, it is possible to calculate the signal-to-noise ratio (SNR) for these regions as ratio of the mean intensity and maximum absolute deviation. The SNR for the substrate region is the same for all samples and equals 17.6 dB while for the NWs it is 15.6, 8.3, 15.4, and 9.4 dB for the as fabricated, dry, wet, and gate samples, respectively. It may seem surprising that the SNR for the substrate

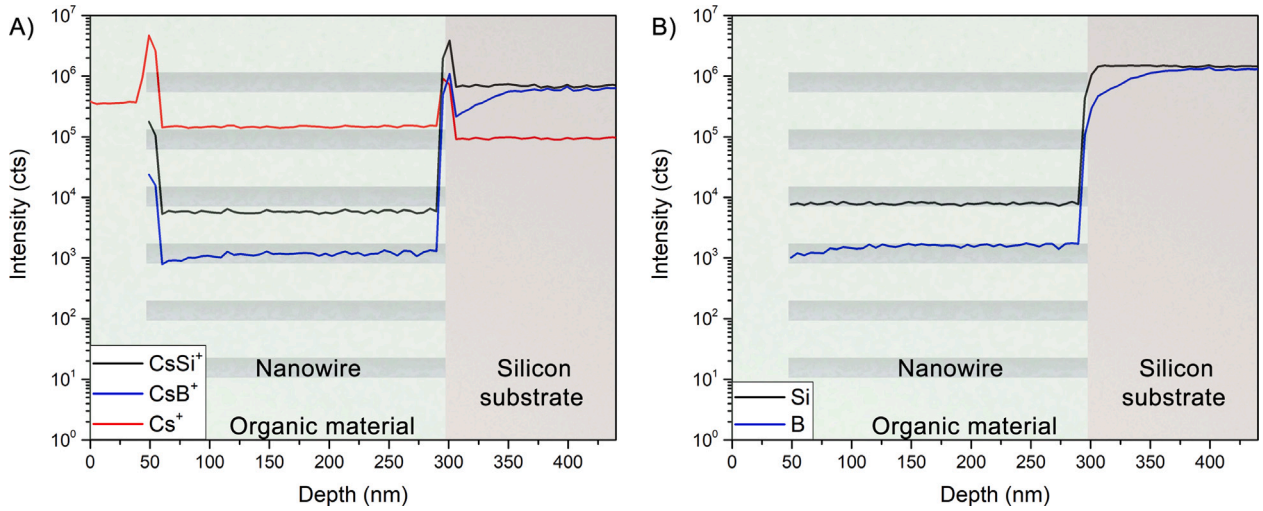

Fig. 3. Depth profiles obtained for the wet sample. Part A: raw data indicate significant agglomeration of cesium at the interface between organic material and silicon. Part B: silicon and boron signals point-to-point normalized to the cesium signal.

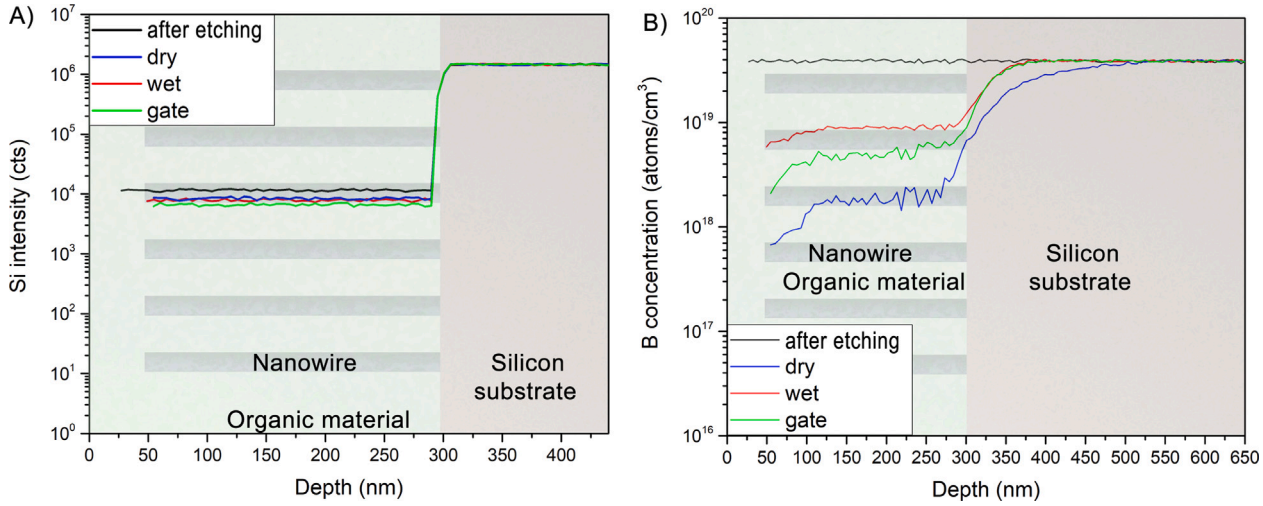

Fig. 4. Part A: Comparison of the silicon signals for all samples. The intensity scales linearly with the total area of the NWs in the array and thus it is possible to determine the diameter of each NW directly from the SIMS measurement. Part B: Comparison of the boron concentrations for all samples. A clear boron depletion is observed after the oxidation processes and subsequent oxide removal.

Table 2
Factor by which the boron concentration in NWs is lower when compared to the sample after etching. The columns show the average value, and the values registered at the tip, middle, and foot of the NWs.

Sample	Average	Tip	Middle	Foot
Dry	21.0	56.7	22.0	5.8
Wet	4.6	6.6	4.5	3.2
Gate	7.9	18.3	9.1	4.3

region is only moderately higher than for the NWs region of the as fabricated sample. It should be, however, noted that the intensity of both, silicon and boron signals in the substrate region is very high (around one million counts per second, as shown in Fig. 3) which is very close to the upper limit of the electron multiplier detector and the error introduced by its dead time is relatively high.

The SNR for the NWs region remains reasonably high for all samples but, as expected, it decreases for samples with lower boron concentration. Further decreases of the boron concentration (either by longer oxidation processes or lower initial dopant level) or NW diameters may result in an unacceptable signal-to-noise ratio. In such a case a larger array of NWs should be fabricated for the SIMS analysis.

4. Conclusions

By embedding the array of vertical nanowires in a photoresist matrix and using a high incident primary ion bombardment makes the measurement procedure to be self-flattening and ensures a uniform sputtering process, despite the difference in the etching rate of both materials. Thus, the proposed method allows the precise quantification of boron distributions in arrays of silicon nanowires with reasonable SNR even for concentration below 10^{18} atoms/cm^3. The sensitivity of the method is directly proportional to the total area of silicon NWs and, thus, it can be expected that for larger arrays (1000 × 1000 NWs) a detection limit of about 5×10^{16} atoms/cm^3 can be achieved with the SNR around 10 dB. This is significantly better than APT analysis can offer. In theory, oxygen primary ions should be more suitable for the analysis of boron dopants. However, preliminary experiments have shown that the differences in the sputtering rate for silicon and

photoresist are not significant and, thus, the analysis will no longer be self-flattening.

The measurement has revealed that during the oxidation of silicon NWs the majority of the boron atoms segregate into the growing oxide and their concentration may decrease even more than one order of magnitude, especially at the tip of the NWs. This change significantly alters the operation of p-type doped GAA-NW-FET devices (Figure S6 in Supplementary Materials) and the knowledge about the non-homogeneous distribution of boron dopants along the height of nanowires may prove invaluable for the further optimization of GAA-NW-FET devices [42].

CRediT authorship contribution statement

Paweł Piotr Michałowski: Conceptualization, Methodology, Validation, Formal analysis, Investigation, Writing – original draft, Writing – review & editing, Visualization, Funding acquisition. **Jonas Müller:** Investigation, Formal analysis, Visualization, Writing – review & editing. **Chiara Rossi:** Software, Data curation, Formal analysis, Visualization, Writing – review & editing. **Alexander Burenkov:** Formal analysis, Writing – review & editing. **Eberhard Bär:** Formal analysis, Writing – review & editing. **Guilhem Larrieu:** Resources, Formal analysis, Writing – review & editing, Supervision. **Peter Pichler:** Conceptualization, Formal analysis, Writing – review & editing, Supervision, Funding acquisition.

Declaration of competing interest

The authors declare that they have no known competing financial interests or personal relationships that could have appeared to influence the work reported in this paper.

Data availability

Data will be made available on request.

Acknowledgments

The research leading to these results has received funding from the European Union's Horizon 2020 research and innovation program under grant agreement No. 871813 MUNDFAB and the National Centre for Research and Development, Poland under grant agreement No. LIDER/8/0055/L-12/20/NCBR/2021. This work was supported by the LAAS-CNRS micro and nanotechnologies platform, a member of the Renatech french national network.

Appendix A. Supplementary data

Supplementary material related to this article can be found online at https://doi.org/10.1016/j.measurement.2023.112630.

References

[1] H.J. Joyce, J.L. Boland, C.L. Davies, S.A. Baig, M.B. Johnston, A review of the electrical properties of semiconductor nanowires: insights gained from terahertz conductivity spectroscopy, Semicond. Sci. Technol. 31 (10) (2016) 103003.
[2] E. Barrigón, M. Heurlin, Z. Bi, B. Monemar, L. Samuelson, Synthesis and applications of III–V nanowires, Chem. Rev. 119 (15) (2019) 9170–9220.
[3] J. Wang, Z. Li, Z. Gu, A comprehensive review of template-synthesized multi-component nanowires: From interfacial design to sensing and actuation applications, Sens. Actuators Rep. 3 (2021) 100029.
[4] L.N. Quan, J. Kang, C.-Z. Ning, P. Yang, Nanowires for photonics, Chem. Rev. 119 (15) (2019) 9153–9169.
[5] C. Jia, Z. Lin, Y. Huang, X. Duan, Nanowire electronics: From nanoscale to macroscale, Chem. Rev. 119 (15) (2019) 9074–9135.
[6] Y. Li, F. Qian, J. Xiang, C.M. Lieber, Nanowire electronic and optoelectronic devices, Mater. Today 9 (10) (2006) 18–27.
[7] F. Patolsky, C.M. Lieber, Nanowire nanosensors, Mater. Today (ISSN: 1369-7021) 8 (4) (2005) 20–28.
[8] S. Mokkapati, C. Jagadish, Review on photonic properties of nanowires for photovoltaics, Opt. Express 24 (15) (2016) 17345–17358.
[9] G. Zhou, L. Xu, G. Hu, L. Mai, Y. Cui, Nanowires for electrochemical energy storage, Chem. Rev. 119 (20) (2019) 11042–11109.
[10] M. Orrù, E. Repiso, S. Carapezzi, A. Henning, S. Roddaro, A. Franciosi, Y. Rosenwaks, A. Cavallini, F. Martelli, S. Rubini, A roadmap for controlled and efficient n-type doping of self-assisted GaAs nanowires grown by molecular beam epitaxy, Adv. Funct. Mater. 26 (17) (2016) 2836–2845.
[11] S. Suomalainen, T.V. Hakkarainen, T. Salminen, R. Koskinen, M. Honkanen, E. Luna, M. Guina, Te-doping of self-catalyzed GaAs nanowires, Appl. Phys. Lett. 107 (1) (2015) 012101.
[12] D. Wolf, H. Lichte, G. Pozzi, P. Prete, N. Lovergine, Electron holographic tomography for mapping the three-dimensional distribution of electrostatic potential in III-V semiconductor nanowires, Appl. Phys. Lett. 98 (26) (2011) 264103.
[13] B. Wu, A. Kumar, S. Pamarthy, High aspect ratio silicon etch: A review, J. Appl. Phys. 108 (5) (2010) 051101.
[14] Z. Huang, N. Geyer, P. Werner, J. de Boor, U. Gösele, Metal-assisted chemical etching of silicon: A review, Adv. Mater. 23 (2) (2011) 285–308.
[15] N.P. Dasgupta, J. Sun, C. Liu, S. Brittman, S.C. Andrews, J. Lim, H. Gao, R. Yan, P. Yang, 25Th anniversary article: Semiconductor nanowires – synthesis, characterization, and applications, Adv. Mater. 26 (14) (2014) 2137–2184.
[16] D.-L. Kwong, X. Li, Y. Sun, G. Ramanathan, Z.X. Chen, S.M. Wong, Y. Li, N.S. Shen, K. Buddharaju, Y.H. Yu, S.J. Lee, N. Singh, G.Q. Lo, Vertical silicon nanowire platform for low power electronics and clean energy applications, J. Nanotechnol. 2012 (2011) 492121.
[17] G. Larrieu, X.-L. Han, Vertical nanowire array-based field effect transistors for ultimate scaling, Nanoscale 5 (2013) 173–176.
[18] X.-L. Han, G. Larrieu, C. Krzeminski, Modelling and engineering of stress based controlled oxidation effects for silicon nanostructure patterning, Nanotechnology 24 (49) (2013) 495301.
[19] T. Kato, Y. Nishi, Redistribution of diffused boron in silicon by thermal oxidation, Japan. J. Appl. Phys. 3 (7) (1964) 377–383.
[20] N. Fukata, S. Ishida, S. Yokono, R. Takiguchi, J. Chen, T. Sekiguchi, K. Murakami, Segregation behaviors and radial distribution of dopant atoms in silicon nanowires, Nano Lett. 11 (2) (2011) 651–656.
[21] S. Koffel, A. Burenkov, M. Sekowski, P. Pichler, D. Giubertoni, M. Bersani, M. Knaipp, E. Wachmann, M. Schrems, Y. Yamamoto, D. Bolze, On an improved boron segregation calibration from a particularly sensitive power MOS process, Phys. Status Solidi C 11 (1) (2014) 12–15.
[22] K. Nomoto, S. Gutsch, A.V. Ceguerra, A. Breen, H. Sugimoto, M. Fujii, I. Perez-Wurfl, S.P. Ringer, G. Conibeer, Atom probe tomography of phosphorus- and boron-doped silicon nanocrystals with various compositions of silicon rich oxide, MRS Commun. 6 (3) (2016) 283–288.
[23] K. Nomoto, H. Sugimoto, A. Breen, A.V. Ceguerra, T. Kanno, S.P. Ringer, I.P. Wurfl, G. Conibeer, M. Fujii, Atom probe tomography analysis of boron and/or phosphorus distribution in doped silicon nanocrystals, J. Phys. Chem. C. 120 (31) (2016) 17845–17852.
[24] Y. Tu, H. Takamizawa, B. Han, Y. Shimizu, K. Inoue, T. Toyama, F. Yano, A. Nishida, Y. Nagai, Influence of laser power on atom probe tomographic analysis of boron distribution in silicon, Ultramicroscopy 173 (2017) 173–176.
[25] K. Wittmaack, High-sensitivity depth profiling of arsenic and phosphorus in silicon by means of SIMS, Appl. Phys. Lett. 29 (1976) 552.
[26] B.Y. Ber, Y.A. Kudriavtsev, A.V. Merkulov, S.V. Novikov, D.E. Lacklison, J.W. Orton, T.S. Cheng, C.T. Foxon, Secondary ion mass spectroscopy investigations of magnesium and carbon doped gallium nitride films grown by molecular beam epitaxy, Semicond. Sci. Technol. 13 (1998) 173–176.
[27] C.Y. Chiou, C.C. Wang, Y.C. Ling, C.I. Chiang, Secondary ion mass spectrometry analysis of in-doped p-type GaN films, Appl. Surf. Sci. 203-204 (2003) 173–176.
[28] M. Emziane, K. Durose, D.P. Halliday, A. Bosio, N. Romeo, In situ oxygen incorporation and related issues in CdTe/CdS photovoltaic devices, J. Appl. Phys. 100 (2006) 013513.
[29] T. Matsunaga, S. Yoshikawa, K. Tsukamoto, Secondary ion yields of C, Si, Ge and Cs surface density and concentration in SIMS, Surf. Sci. 515 (2002) 173–176.
[30] H. Gnaser, SIMS detection in the 10^{12} atoms cm^{-3} range, Surf. Interface Anal. 25 (1997) 173–176.
[31] K. Wittmaack, W. Wach, Profile distortions and atomic mixing in SIMS analysis using oxygen primary ions, Nucl. Instrum. Methods Phys. Res. 191 (1) (1981) 327–334.
[32] J.B. Clegg, A.E. Morgan, H.A.M. de Grefte, F. Simondet, A. Huber, G. Blackmore, M.G. Dowsett, D.E. Sykes, C.W. Magee, V.R. Deline, A comparative study of SIMS depth profiling of boron in silicon, Surf. Interface Anal. 6 (4) (1984) 162–166.
[33] W. Vandervorst, F.R. Shepherd, R.G. Downing, High resolution SIMS and neutron depth profiling of boron through oxide–silicon interfaces, J. Vac. Sci. Technol. A 3 (3) (1985) 1318–1321.
[34] B. Gautier, J. Dupuy, B. Semmache, G. Prudon, SIMS depth profile correction for the study of the first step of the diffusion of boron in silicon, Nucl. Instrum. Methods Phys. Res. B 142 (3) (1998) 361–376.

[35] L. Shao, J. Liu, C. Wang, K.B. Ma, J. Zhang, J. Chen, D. Tang, S. Patel, W.-K. Chu, Response function during oxygen sputter profiling and its application to deconvolution of ultrashallow b depth profiles in Si, Appl. Phys. Lett. 83 (26) (2003) 5467–5469.

[36] A. Merkulov, P. Peres, S. Choi, F. Desse, M. Schuhmacher, Advanced SIMS quantification in the first few nm of B, P and As ultrashallow implants, Surf. Interface Anal. 43 (1–2) (2011) 522–524.

[37] A. Merkulov, P. Peres, K. Soulard, D.J. Larson, K. Sivaramakrishnan, Improvement of extra low impact energy SIMS data reduction algorithm for process control, J. Vac. Sci. Technol. B 38 (5) (2020) 053201.

[38] C.N.S. Kumar, S. Tabean, A. Morisset, P. Wyss, M. Lehmann, F.-J. Haug, Q. Jeangros, A. Hessler-Wyser, N. Valle, T. Wirtz, S. Eswara, Evaluation of secondary electron intensities for dopant profiling in ion implanted semiconductors: a correlative study combining SE, SIMS and ECV methods, Semicond. Sci. Technol. 36 (8) (2021) 085003.

[39] X.-L. Han, G. Larrieu, P.-F. Fazzini, E. Dubois, Realization of ultra dense arrays of vertical silicon nanowires with defect free surface and perfect anisotropy using a top-down approach, Microelectron. Eng. (ISSN: 0167-9317) 88 (8) (2011) 2622–2624, proceedings of the 36th International Conference on Micro- and Nano-Engineering (MNE).

[40] Y. Guerfi, F. Carcenac, G. Larrieu, High resolution HSQ nanopillar arrays with low energy electron beam lithography, Microelectron. Eng. (ISSN: 0167-9317) 110 (2013) 173–176.

[41] G. Larrieu, Y. Guerfi, X. Han, N. Clément, Sub-15 nm gate-all-around field effect transistors on vertical silicon nanowires, Solid-State Electron. (ISSN: 0038-1101) 130 (2017) 173–176.

[42] C. Rossi, A. Burenkov, P. Pichler, E. Bär, J. Müller, G. Larrieu, Performance of vertical gate-all-around nanowire p-MOS transistors determined by boron depletion during oxidation, Solid-State Electron. 200 (2023) 108551.